

# Flow and sediment dynamics in bed discordant channel confluences

**Koen BLANCKAERT**

*State Key Laboratory of Urban and Regional Ecology, Research Center for Eco-Environmental Sciences, Chinese Academy of Sciences, Beijing, China*  
*Laboratory of Hydraulic Constructions (LCH). Ecole Polytechnique Fédérale de Lausanne (EPFL), Station 18, Lausanne, Switzerland*

**Marcelo LEITE RIBEIRO**

*Laboratory of Hydraulic Constructions (LCH). Ecole Polytechnique Fédérale de Lausanne (EPFL), Station 18, Lausanne, Switzerland*  
*Stucky SA. Renens, Switzerland*

**Anton J. SCHLEISS**

*Laboratory of Hydraulic Constructions (LCH). Ecole Polytechnique Fédérale de Lausanne (EPFL), Station 18, Lausanne, Switzerland*

**ABSTRACT:** Confluences between small steep tributaries with dominant supply of poorly sorted sediment and larger main channels with dominant flow supply, which are characterized by a pronounced bed discordance, have not yet been considered in the literature. The hydro-morpho-sedimentary processes in such confluences are not well described by existing conceptual models of confluence dynamics. Examples of such confluences on the Upper Rhone River, Switzerland, served as prototype for the reported laboratory experiments. Based on detailed measurements of the morphology, the sediment size, the sediment transport, and the three-dimensional flow field in a laboratory experiment, Leite Ribeiro, et al. (submitted) have proposed a conceptual model for the hydro-morpho-sedimentary processes in the investigated type of confluences. According to this model, the pronounced bed discordance is essentially due to the difference between the low flow depth in the steep tributary and the higher flow depth in the main channel. The tributary flow penetrates into the main channel mainly in the upper part of the water column. Due to the bed discordance, the main-channel flow is hardly hindered by the tributary in the lower part of the water column, giving rise to a two-layer flow structure at the tributary mouth. In confluences with dominant sediment supply from the tributary, the development of a deposition bar downstream of the confluence reduces the flow area and causes a flow acceleration that contributes to the required increase in sediment transport capacity. The sediment supplied by the tributary is mainly sorted and transported on the sloping face of the depositional bar. The sediment transport capacity is further increased by the three-dimensionality of the flow, which is characterized by maximum velocities occurring near the bed. The present paper reports data on the morphology and flow visualizations for two additional hydrological scenario, characterized by different flow ratios, but an identical sediment supply in the tributary. An increase in the ratio of tributary discharge to main-channel discharge led to an attenuation of the morphological features in the confluence zone: (i) the bed discordance was less pronounced; (ii) the tributary penetration was reduced; (iii) the volume of sediment accumulated in the depositional bar just downstream of the confluence decreased. Leite Ribeiro et al. 's (submitted) conceptual model is able to explain these morphological adaptations, which lends credit to the robustness of their model.

## 1 INTRODUCTION

*Stucky SA. Renens, Switzerland* Confluences cause significant changes in flow dynamics, sediment transport and bed morphology, which are known to depend on the confluence characteristics. This paper investigates the hydro-morpho-sedimentary processes of confluences in rivers such as the Upper Rhone River, upstream of Lake Geneva, Switzerland. This river and its tributaries are channelized at an almost constant embanked width. The confluences are characterized by pronounced bed discordances (i.e. the difference in bed elevation between the tributary and the main channel at the tributary mouth), which have often been stabilized by means of weirs or block ramps. A major river rehabilitation project is at present in progress, which aims at conciliating improved flood protection and enhanced ecological value. The rehabilitation of confluence zones, which is an important component of the overall rehabilitation project, is hindered by a lack of understanding of the relevant hydro-morpho-sedimentary processes.

These processes are known to depend on the confluence configuration, including the planform and slope of the adjoining channels, confluence angle, discharge and momentum flux ratios, bed material and sediment supply. Leite Ribeiro et al. (submitted) have summarized the foregoing investigations on confluence morphodynamics and concluded that the current understanding is based on a surprisingly small number of investigated configurations, as represented by the conceptual models of Best (1988) based on laboratory experiments, Boyer et al. (2006) based on investigations on the Bayonne-Berthier confluence and Rhoads et al. (2009) based on investigations on the confluence of the Kaskaskia River and Copper Slough. Due to considerably different confluence characteristics, none of these conceptual models can represent the hydro-morpho-sedimentary processes in confluences on the Upper Rhone River. Based on detailed measurements of the morphology, the sediment size, the sediment transport, and the three-dimensional flow field in a laboratory experiment, (Leite Ribeiro, et al., submitted) have proposed a conceptual model for confluences such as those on the Upper Rhone River, that have the following characteristics:

- The main channel provides the dominant discharge, as quantified by the discharge ratio  $Q_t/Q_m$  and momentum flux ratio  $M_r = \rho Q U_t / \rho Q U_m$ .  $Q$  [ $\text{m}^3 \text{s}^{-1}$ ] is the discharge,  $\rho$  [ $\text{kgm}^{-3}$ ] is the water density,  $U$  [ $\text{ms}^{-1}$ ] is the mean velocity and the subscripts  $t$  and  $m$  represents the tributary and main channels, respectively.
- The sediment is predominantly and abundantly supplied by the tributary, and consists of poorly-sorted gravel.
- The steep tributary is smaller than the main low-gradient channel. The flow in the tributary is transcritical during formative floods, i.e. the Froude number is close to unity.

Because this model will serve as reference in the present investigation on the influence of the discharge ratio  $Q_t/Q_m$  and the momentum flux ratio  $M_r = \rho Q U_t / \rho Q U_m$ , its main features will now briefly be described (Figure 1). The pronounced bed discordance ( $M1$ ) at the confluence mouth is due to the important difference between the flow depths in the steep tributary and in the low-gradient main channel. The formation of a stagnation zone ( $F4$ ) at the upstream confluence corner causes an asymmetric distribution of the flow and sediment transport, whereby the sediment transfer between the tributary and the main channel mainly occurs near the downstream corner of the confluence. The presence of a large depositional sediment bar at the inner bank ( $M2$ ) and the absence of a marked scour hole at the outer bank ( $M5$ ) are typical for confluences characterized by a dominant and abundant sediment supply originating from the tributary and low discharge and momentum flux ratios. The depositional sediment bar leads to a reduction in cross-sectional area and a corresponding acceleration of the flow that provides the increase in sediment transport capacity, which allows the load from the tributary to be transported through the confluence zone. The pronounced bed discordance leads to the formation of a two-layer flow structure in the confluence zone ( $F1, F2, F3$ ). Flow originating from the tributary mainly protrudes in the upper part of the water column of the main channel, where it forms an obstruction for flow originating from the main channel and deviates the latter outwards. The bed discordance protects the flow in the lower part of the water column from the obstruction by the tributary inflow, and allows it to go straight on. The two-layer flow structure does not lead to the formation of secondary flow circulation cells. The near-bed flow originating from the main channel encounters at the confluence mouth coarse sediment supplied by the tributary. This near near-bed flow is mainly found on the sloping faces of the depositional sediment bar ( $M3$ ). It accelerates and has a component that is directed upwards the slope of the depositional bar. This

component equilibrates the downslope gravitational pull on the sediment particles and thereby conditions the slope of the depositional bar's face and the sediment sorting occurring on them. A shear layer ( $F5$ ) develops where flows originating from the tributary and from the main channel collide. It is characterized by increased turbulence and its outer limit coincides closely with the toe of the sediment bar ( $M2$ ). In the downstream confluence corner, spiral vortices ( $F6$ ) lift fine material into suspension. Fine materials are then transported near the inner bank ( $M4$ ) while the coarse ones are transported on the face of the depositional bar ( $M3$ ). Leite Ribeiro et al. (submitted) report a detailed discussion of the similarities and differences of this conceptual model to aforementioned conceptual models developed for configurations with different characteristics.

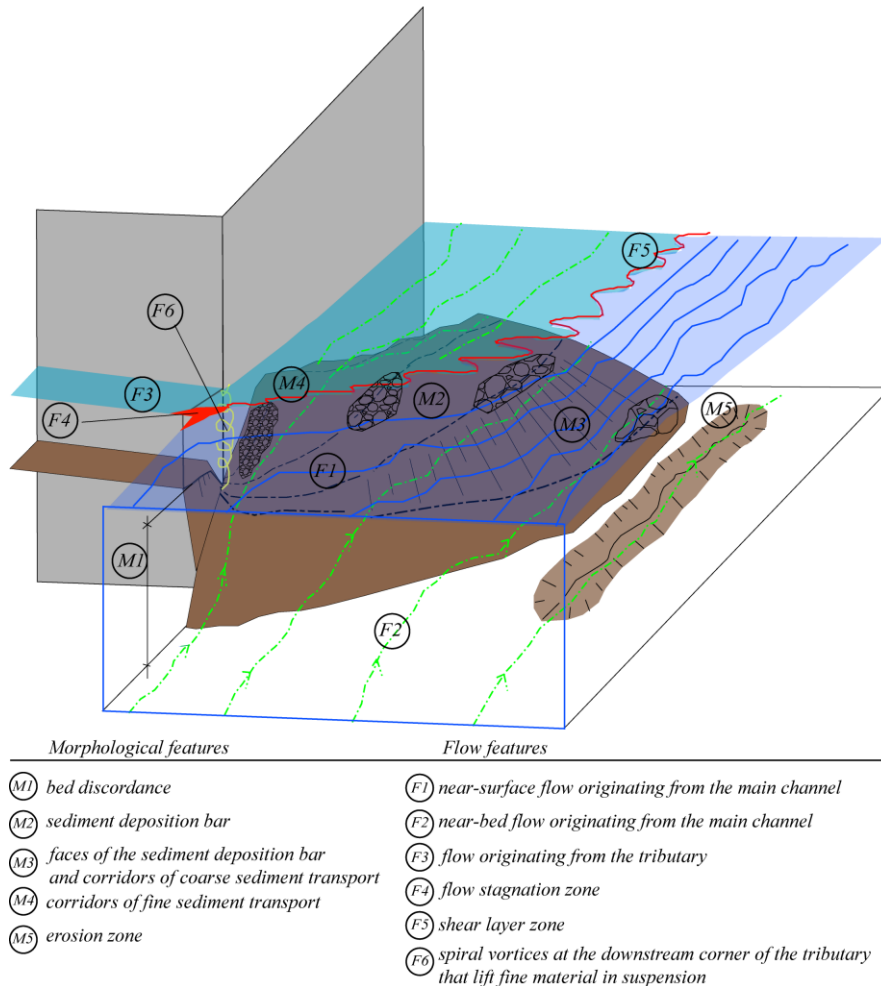


Figure 1 Conceptual model for hydro-morpho-sedimentary processes in confluences between a small steep tributary with dominant supply of poorly sorted sediment and a larger low-gradient main channel with dominant flow supply (Leite Ribeiro, et al., submitted for publication)

This paper reports an investigation in a laboratory setting that is representative of the 20 major confluences on the Upper Rhone River, which the aim of:

- Providing detailed experimental data on the flow and the morphology in a reference configuration (which is reported in more detail by Leite Ribeiro et al.) as well as data on the morphology and flow visualizations in two additional configurations with different scenarios of the discharge ratio  $Q_t/Q_m$  and the momentum flux ratio  $M_r = \rho Q U_t / \rho Q U_m$ .
- Analyzing the hydro-morpho-sedimentary implications of these different hydrological scenarios.
- Evaluating the robustness of the Leite Ribeiro et al.'s (submitted) conceptual model (Figure 1) for the hydro-morpho-sedimentary processes.

## 2 THE EXPERIMENTS

The experimental design of the reported experiments, including the confluence geometry, the sediment characteristics and the flow and sediment discharges, is inspired by the confluences on the Upper Rhone River upstream of Lake Geneva, Switzerland. The experimental set-up is not a scale model of one particular confluence, but rather a schematized configuration that aims at mimicking the dominant hydro-morpho-sedimentary processes occurring in a broader range of configurations with the specific characteristics mentioned in the introduction.

Table 1 presents a summary of the geometric and hydraulic characteristics of the Upper Rhone's 20 main confluences;  $B$  is the channel width,  $Q_2$  and  $Q_5$  represent the two and five year return period floods (adopted as formative floods), respectively and the subscripts  $t$ ,  $m$  and  $p-c$  represents the tributary, main and post-confluence channels respectively (Figure 2). The Froude numbers at the tributary ( $Fr_t$ ) and the momentum flux ratios ( $M_r$ ) between the tributary and the main channels estimated for  $Q_2$  and  $Q_5$  are also shown in Table 1.

Table 1 Geometric and hydraulic characteristics of the Upper Rhone River's (Switzerland) 20 main confluences

	Angle [°]	$B_t/B_m$	$B_m/B_{p-c}$	Tributary bed slope [%]	$Q_{2,t}/Q_{2,m}$	$Q_{5,t}/Q_{5,m}$	$Fr_{tQ_2}$	$Fr_{tQ_5}$	$M_{r-Q_2}$	$M_{r-Q_5}$
<b>Average</b>	62	0.22	1.02	1.1%	0.10	0.09	0.83	0.83	0.11	0.08
<b>Max</b>	90	0.54	1.27	4.0%	0.32	0.31	1.29	1.30	0.45	0.30
<b>Min</b>	30	0.07	0.71	0.0%	0.01	0.01	0.03	0.03	0.01	0.01

The experimental facility consists of a flume with smooth vertical banks where the main channel is 8.5 m long and 0.50 m wide. The 4.9 m long and 0.15 m wide tributary channel is connected at an angle of 90° to the main channel 3.60 m downstream of the inlet (Figure 2). The results in this paper are represented in the ( $X, Y, Z$ ) reference system represented in Figure 2.

Although the intersection angles of the tributaries with the upper Rhone River are highly variable (Table 1), the maximum value of 90° was adopted and kept constant in the reported experiments. The ratio of the tributary width to the main channel width of  $B_t/B_m = 0.3$  and of the main channel width to the post-confluence channel width of  $B_m/B_{p-c} = 1$  are representative of the confluences in the Upper Rhone River.

Leite Ribeiro et al. (submitted) investigated a so-called "low-discharge" hydrological scenario where the flow discharges in the main channel and the tributary were constant at  $Q_m = 18 \text{ l s}^{-1}$  and  $Q_t = 2 \text{ l s}^{-1}$ , respectively, leading to a discharge ratio of  $Q_t/Q_m = 0.11$ , and a momentum flux ratio of  $M_r = \rho Q U_t / \rho Q U_m = 0.20$ . The present paper reports two additional flow scenario, a so-called "intermediate-discharge" scenario with  $Q_t = 2.6 \text{ l/s}$  and  $Q_m = 17.4 \text{ l/s}$  ( $Q_t/Q_m = 0.15$  and  $M_r = 0.27$ ) and so-called "high-discharge" scenario with  $Q_t = 3.7 \text{ l/s}$  and  $Q_m = 16.3 \text{ l/s}$  ( $Q_t/Q_m = 0.23$  and  $M_r = 0.49$ ). In all scenarios, flow was rough turbulent,  $Re_* = u_* k_s / \nu > 70$ , where  $Re_*$  represents the particle Reynolds number,  $u_*$  the shear velocity defined as  $u_* = (g H E_s)^{1/2} \text{ [m s}^{-1}\text{]}$  with  $H$  and  $E_s$  the average flow depth and the energy gradient,  $k_s \text{ [m]}$  the characteristic particle size and  $\nu \text{ [m}^2 \text{ s}^{-1}\text{]}$  the kinematic viscosity.

The sediment characteristics satisfy three requirements: (i) they yield a longitudinal slope in the tributary that is in the range of those presented in Table 1 ; (ii) they yield a Froude number in the tributary that is close to unity; (iii) their grain size distribution is representative of the Upper Rhone. Poorly-sorted sediments with  $d_{50} = 0.8 \text{ mm}$ ,  $d_m = 2.3 \text{ mm}$   $d_{90} = 5.7 \text{ mm}$  and a sorting coefficient of  $\sigma = 0.5 (d_{84}/d_{50} + d_{50}/d_{16}) = 4.15$ , were used for the bed material and the solid discharge. The particle size distribution of the sediment is shown in Figure 2.

A constant sediment discharge is only supplied to the tributary and there is no sediment supply to the main channel. This procedure aims at reproducing conditions where the main channel's bed is armored and its banks are protected, and where floods in the steep tributary carry important loads of sediment. Such conditions occur in the Upper Rhone River. The bed was initially covered with the poorly sorted sediment mixture in the main channel and the tributary. The initial bed was flat in the main and post-confluence channels and had a longitudinal slope of around 0.05% in the tributary near its mouth. Steady flow discharges were provided to the main channel and the tributary, respectively, and a constant solid discharge of 0.3 kg/min was fed to the tributary. An adjustable tailgate at the end of the post-confluence channel controlled the flow depth within the entire flume. The water level at the

downstream boundary of the flume was kept constant at 0.07 m. During the experiment, sediment volumes entering and leaving the flume were weighed. Achievement of equilibrium was assessed on the basis of changes in the bed morphology and of the sediment budget.

Water levels and bed topography were measured during the experiments with ultrasonic gauges and a Mini EchoSounder, respectively. Instruments were installed on a movable frame that covered a region of 3.80 m by 3.00 m in the confluence zone as shown in Figure 2. Upstream flow discharges were accurately measured by means of a calibrated V-notch weir on the main channel and an electromagnetic flow meter on the tributary channel, respectively. At the end of the experiment, the surface bed material was sampled at four different locations (S1, S2, S3 and S4 shown in Figure 2) and grain size analysis by means of hand sieving was carried out.

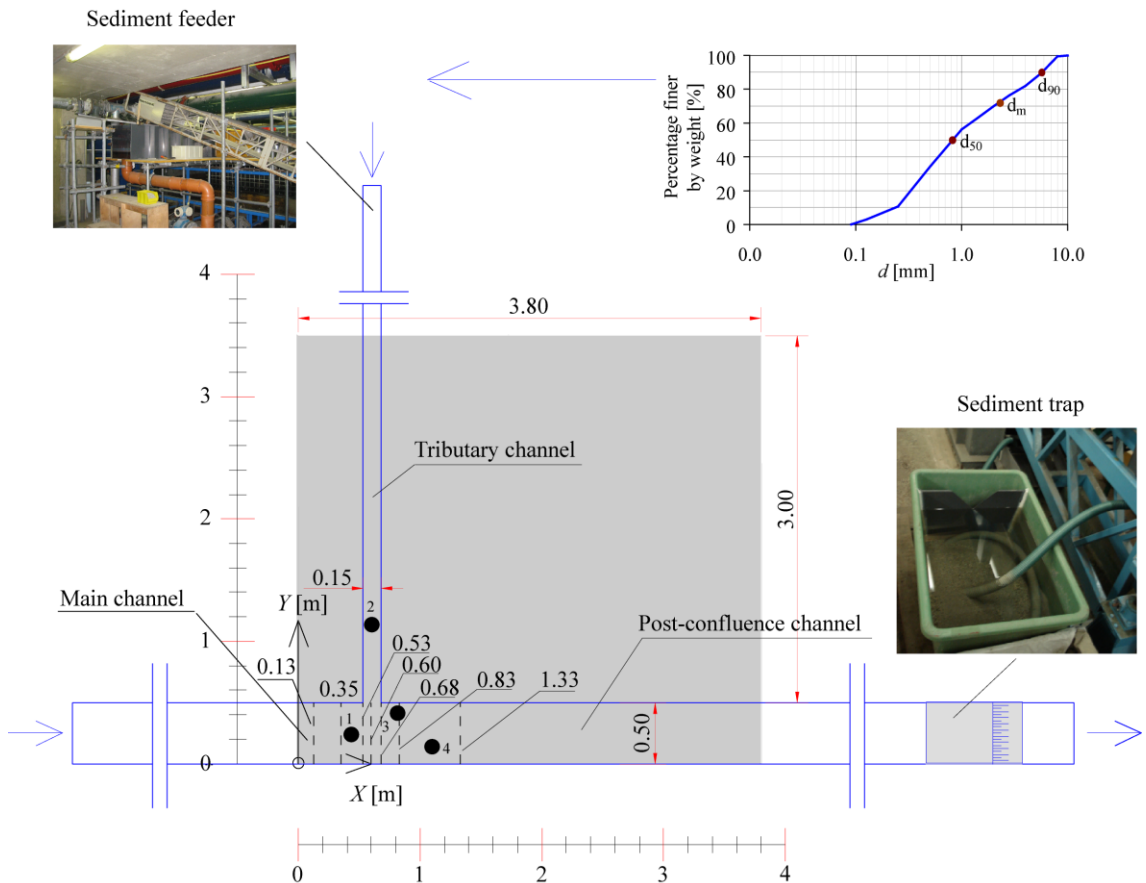


Figure 2 Experimental facility and particle size distribution of the sediment. The locations of the cross sections where velocity measurements were performed are indicated by the dashed lines and the locations of the bed samples by the dark circles. The limit between the main channel and the post-confluence channel is the tributary axis at  $X = 0.60$  m

Velocity measurements were only performed for the “low-discharge” scenario. Vertical profiles of the three velocity components were measured with high temporal resolution by means of an Acoustic Doppler Velocity Profiler (ADVP) developed at École Polytechnique Fédérale Lausanne, Switzerland, as detailed in Leite Ribeiro et al. (submitted). The working principle of the ADVP has been reported by Hurther and Lemmin (1998), Blanckaert and Graf (2001) and Blanckaert and Lemmin (2006). Blanckaert (2010) describes in detail the working principle as well as the data treatment procedures. He quantified the uncertainty in the measurement of the mean flow and turbulent flow quantities, which can be summarized as follows: about 4% in the time-averaged streamwise velocity  $u_x$ , and about 10 % in the cross-stream velocities ( $u_y, u_z$ ).

### 3 BED MORPHOLOGY

The equilibrium bed morphologies for the three flow scenarios are shown in Figure 3. The main morphological features resulting from the different discharge scenarios are similar and in agreement with the conceptual model presented in the Introduction (Figure 1). Nevertheless, important differences concerning the magnitude of the bed discordance, tributary penetration, deposition bar and erosion zone can be highlighted.

The equilibrium bed morphologies in the post-confluence channel are characterized by the formation of a substantial depositional bar near the inner bank which attains its maximum height just downstream of the confluence (Figure 3,

Figure 4). A corridor of fine sediment transport near the inner bank is associated with a small depression in the post-confluence channel (Figure 3).

With increase of the discharge, the volume of the sediment bar reduces and the deposits are shifted towards downstream. At the center of the main and post-confluence channels the longitudinal profile of the depositional bar is similar for all tests (Figure 3,

Figure 4). The presence of the depositional bar causes a reduction in the cross-sectional area downstream of the confluence, which is accompanied by an increase in the energy gradient and an acceleration of the flow. These features cause some slight erosion near the outer bank just downstream of the confluence (Figure 3,

Figure 4), which slightly increases with the increase of the discharge ratio.

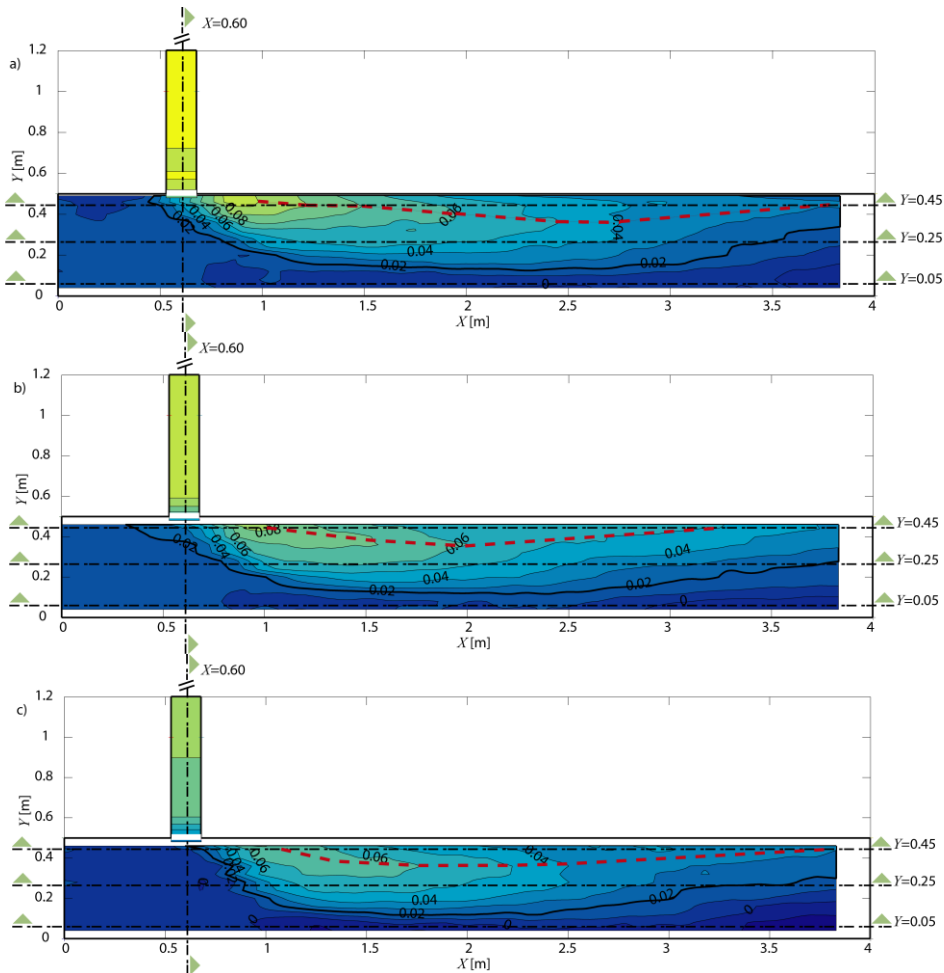


Figure 3 Equilibrium bathymetry for the three flow scenarios. Contour lines denote the bed elevation,  $Z$ [m]. The red dashed lines represent the crest of the depositional bar; the thick black line indicates the initial bed level

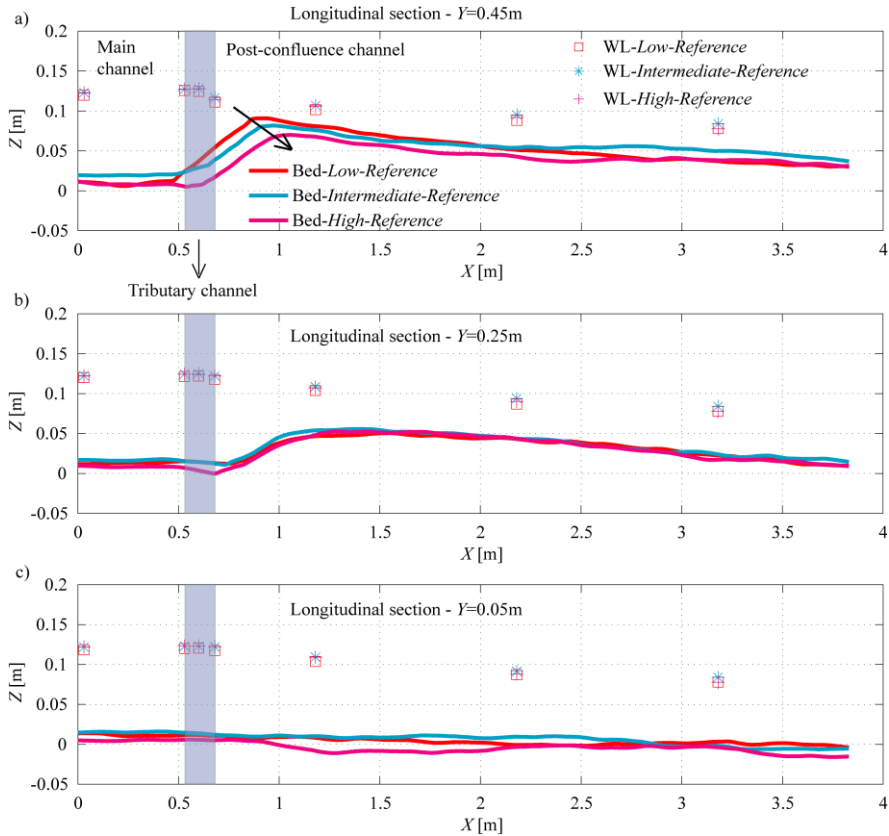


Figure 4 Longitudinal profiles of the main and post-confluence channels at a)  $Y=0.45$  m, b)  $Y=0.25$  m and c)  $Y=0.05$  m showing the water levels and bed elevations for the three flow scenarios

Because the solid discharge and the composition of the sediment input material are identical in all three scenarios, the increase of the tributary discharge leads to an increase of the tributary flow depth ( $H_t=0.02$  m, 0.026 m and 0.04 m respectively for the low, intermediate and high discharges) and a reduction of the equilibrium tributary bed slope ( $S_t \sim 1.9\%$ , 1.5% and 1.2% respectively for the low, intermediate and high discharge scenarios). Therefore, bed discordance decreases with increasing discharge ratio (Figure 5), which is in accordance with the conceptual model (Figure 1). Another important observation is related to the tributary penetration into the main channel, which decreases with increasing discharge ratio (Figure 3). Increasing the discharge ratio leads to an increase of the discharge that is confined near the inner bank by the main channel flow, which leads to an increase in the sediment transport capacity near the confluence mouth. This explains the reduction of the tributary penetration and of the sediment volume in the bar observed with increasing discharge ratio.

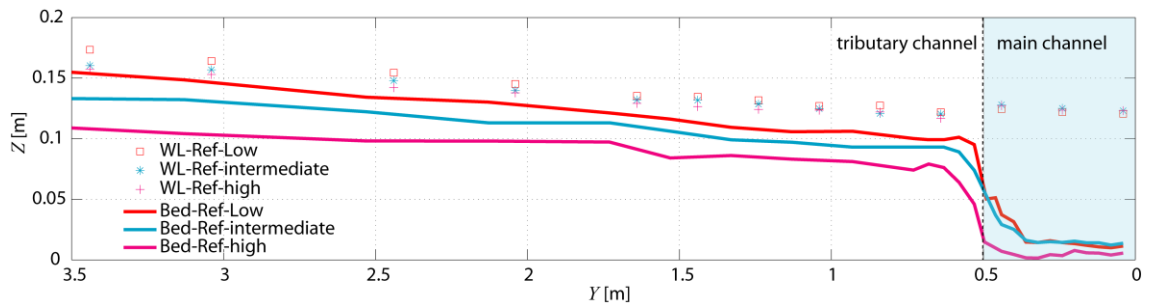


Figure 5 Longitudinal profiles of the tributary channel at  $X=0.60$  m showing the water and bed elevations for the three flow scenarios

## 4 FLOW DYNAMICS

### 4.1 Flow visualization

According to the conceptual model (Figure 1), the lateral expansion of the depositional bar about coincides with the outer limit of the shear layer that is formed by the collision of the flow originating from the main channel and the tributary. Interestingly, the increased discharge ratio does neither lead to a considerable widening of the depositional bar, nor to a considerable outwards shift of the shear layer (Figure 6). This indicates that the system is mainly determined by the sediment input, which conditions the morphology in the confluence zone and the post-confluence channel (where the solid and water discharges are the same for all three scenarios). The morphology, on its turn, determines the position of the shear layer as well as the global flow distribution.

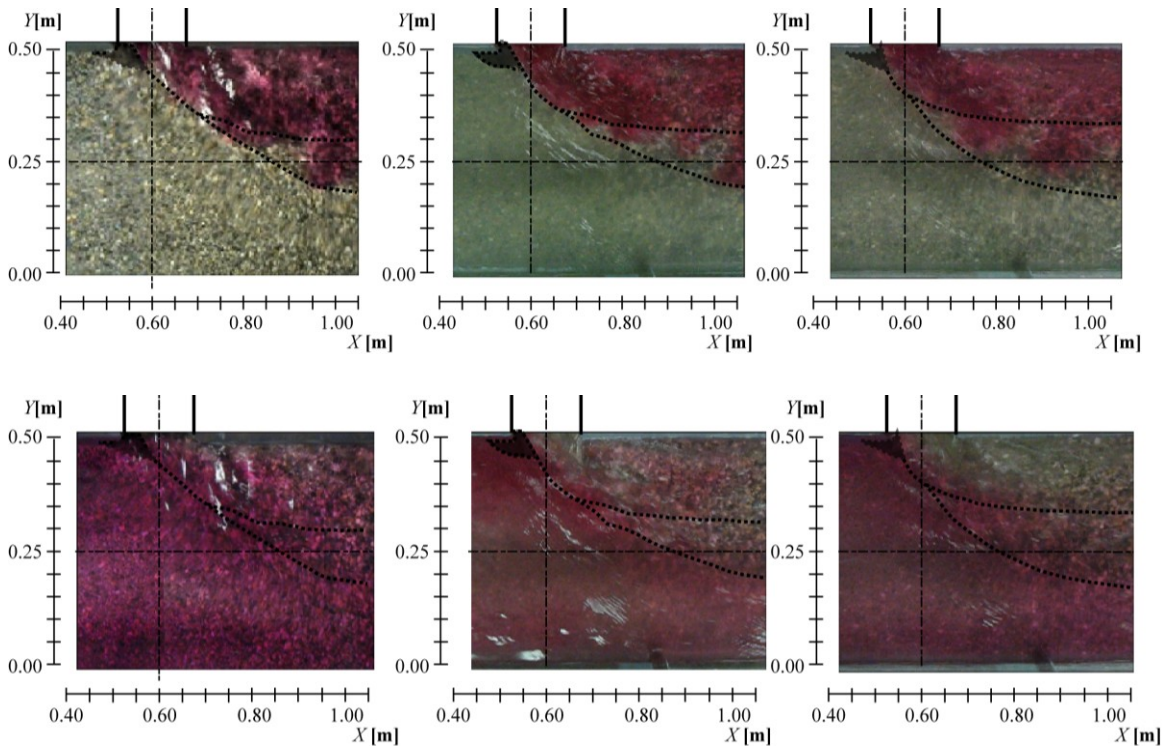


Figure 6 Flow visualization of the confluence zone for the three investigated flow scenario; (left) “low discharge” scenario; (middle) “Intermediate discharge” scenario; (right) “high discharge” scenario. Color dye is injected: (top row) only in the tributary; (bottom row) only in the main channel. The approximate flow stagnation zone and the limits of the shear layer zone are shown by the dashed lines

The behavior of the two-layer flow (see Figure 1) due to the presence of the bed discordance is considerably modified with the increasing discharge ratios. The “low-discharge” scenario leads to the lowest momentum flux ratio and the highest bed discordance. The bed discordance protects the flow originating from the main channel in the lower part of the water column from the obstruction by the tributary inflow, and allows it to go straight on (Figure 1, Figure 6). The increase of the tributary flow (and decrease of the main channel flow) leads to smaller bed discordance and a higher momentum flux ratio. Therefore, the main channel near-bed flow is more influenced by the tributary momentum input and its deflection towards the outer bank of the post-confluence channel increases (Figure 6).

The two-layer flow structure in the confluence zone is further illustrated in the following sections by means of detailed flow measurements performed in the “low-discharge” flow scenario. A detailed discussion of the measured patterns of mean flow and turbulence, as well as their interaction with the morphology is reported in Leite Ribeiro et al. (submitted).



#### 4.2 The three-dimensional flow field

The two-layer flow structure is clearly discernable in Figure 7, which shows a zoom of the bed topography in the confluence zone as well as the near-bed and the near-surface flow velocities at  $Z/h = 0.2$  (dashed vectors) and  $Z/h = 0.7$  (full vectors), respectively, in the experiment with “low-discharge” scenario. At the tributary mouth, the near-bed flow from the main channel follows a rather straight path that is directed upwards the slope of the depositional bar (most left near-bed vector in  $X = 0.60$  and  $X = 0.83$ ; Figure 7). The presence of the tributary flow in this zone can be easily recognized by the near surface velocities that are outwards directed and, which deviate the flow originating from the main channel to the outer bank (full ellipse). Outside of the zone occupied by the depositional bar (dashed ellipse), the near-bed flow is about parallel to the depositional bar contourlines while the near-surface flow is slightly less outwards skewed. The vertical skewing of the velocity profile does not lead to the formation of helical flow cells, however, since no upward/downward vertical velocities occur that are of similar magnitude to the variation of the transverse velocity component over the flow depth (Figure 8).

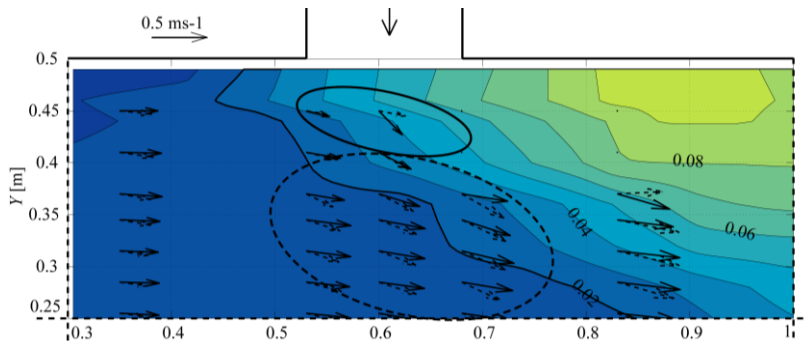


Figure 7 Zoom of the equilibrium bed topography in the confluence zone with the vectors  $(u_x, u_y)$  near the bed at  $Z/h = 0.2$  (dashed vectors) and near the surface at  $Z/h = 0.70$  (full vectors) in the experiment with “low-discharge” scenario

Figure 8 shows the vectors of the cross-sectional velocities  $(u_y, u_z)$  superimposed on the contours of the streamwise velocity  $u_x$  in the cross-section at the downstream tributary corner ( $X = 0.68\text{m}$ ) in the experiment with “low-discharge” scenario. The pronounced transverse velocities near the inner bank represent the transverse inflow from the tributary. They follow the bed topography and weaken with distance from the inner bank, which is due to the change in the direction of flow (see visualization in Figure 6). The momentum input by the tributary increases the magnitude of the velocity vector near the inner bank (Figure 7) and causes the core of highest velocity magnitudes to occur near the inner bank close to the bed. This core of highest velocities is of particular importance for the transport of sediment originating from the tributary. Velocities near the inner bank are smallest at the water surface and increase considerably towards the bed, confirming the two-layer structure of the flow at this location.

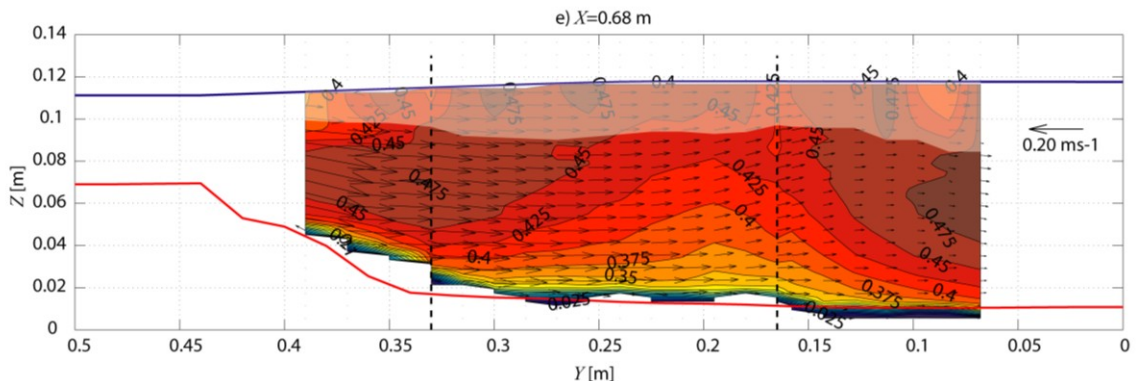


Figure 8 Mean streamwise flow velocities  $u_x$  (contours) and cross-sectional velocities,  $(u_y, u_z)$  (vectors) in the cross-section at the downstream tributary corner ( $X = 0.68\text{m}$ ) in the experiment with “low-discharge” scenario. The shaded areas indicate regions where the flow measurements are perturbed by the ADVP housing that touches the water surface (more details in (Blanckaert, 2010))

## 5 DISCUSSION AND CONCLUSIONS

This paper examined confluences that are characterized by small steep tributaries with high supply of poorly sorted sediment that join the main channel under relatively low discharge and momentum flux ratios. These characteristics condition the hydro-morpho-sedimentary processes, which differ from existing conceptual models of Best (1988), Boyer et al. (2006) and Rhoads et al. (2009) for confluences with different characteristics. Based on detailed measurements of the morphology, the sediment size, the sediment transport, and the three-dimensional flow field in a laboratory experiment, Leite Ribeiro, et al. (submitted) have proposed a conceptual model for the hydro-morpho-sedimentary processes in the investigated type of confluences. The present paper reported data on the morphology and flow visualizations for two different hydrological scenarios, characterized by different flow ratios, but an identical sediment supply in the tributary. An increase in the ratio of tributary discharge to main-channel discharge led to an attenuation of the morphological features in the confluence zone: (i) the bed discordance was less pronounced; (ii) the tributary penetration was reduced; (iii) the volume of sediment accumulated in the depositional bar just downstream of the confluence decreased. Leite Ribeiro et al. 's (submitted) conceptual model is able to explain these morphological adaptations, which lends credit to the robustness of their model.

## 6 ACKNOWLEDGEMENTS

The research was supported by the Swiss Federal Office for the Environment (FOEN) in the framework of the project "Integrated management of river systems". The second author was partially funded by the Chinese Academy of Sciences fellowship for young international scientists under Grant No. 2009YA1-2 and by the Sino-Swiss science and technology cooperation for joint research, project GJH20908.

## REFERENCES

- Best, J. L. (1988), Sediment transport and bed morphology at river channel confluences, *Sedimentology*, 35, 481-498.
- Blanckaert, K. (2010), Topographic steering, flow recirculation, velocity redistribution, and bed topography in sharp meander bends, *Water Resour. Res.*, 46, W09506.
- Blanckaert, K., and W. H. Graf (2001), Mean Flow and Turbulence in Open-Channel Bend, *Journal of Hydraulic Engineering*, 127, 835-847.
- Blanckaert, K., and U. Lemmin (2006), Means of noise reduction in acoustic turbulence measurements, *Journal of Hydraulic Research*, 44, 3-17.
- Boyer, C., A. G. Roy, and J. L. Best (2006), Dynamics of a river channel confluence with discordant beds: Flow turbulence, bed load sediment transport, and bed morphology, *Journal of Geophysical Research*, 111, 1-22.
- Hurther, D., and U. Lemmin (1998), A constant-beam-width transducer for 3D acoustic Doppler profile measurements in open-channel flows, *Meas. Sci. Technol.*, 9, 1706-1714.
- Leite Ribeiro M, Blanckaert K, Roy AG and Schleiss AJ, Flow and sediment dynamics in channel confluences, submitted to *Journal of Geophysical Research*.
- Rhoads, B. L., J. D. Riley, and D. R. Mayer (2009), Response of bed morphology and bed material texture to hydrological conditions at an asymmetrical stream confluence, *Geomorphology*, 109, 161-173.